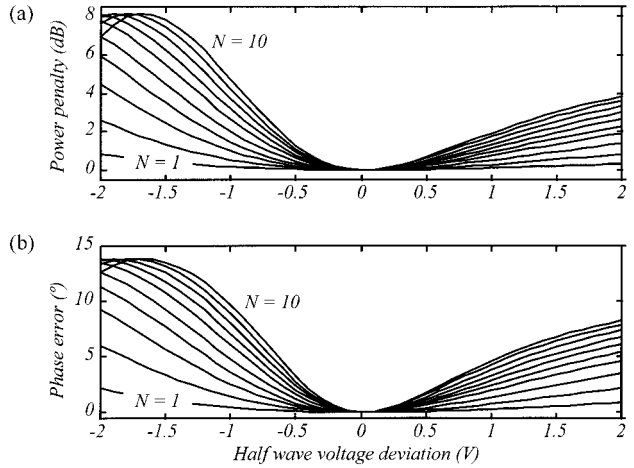

Figure 3 Effects of MZ–EOM half-wave voltage deviations on: (a) power penalty, (b) phase-shift error. N is the LO harmonic order

($N = 1 \ldots 10$). While keeping the $V_\pi(f_{LO})$ deviation below ± 0.5 V, the power penalty is less than 1.5 dB, and the phase error remains below 3°. The limitations caused by $V_\pi(f_{IF})/V_\pi(f_{RF})$ deviations may be neglected as they correspond to the $N = 1$ case, in which a significant $V_\pi(f_{IF})/V_\pi(f_{RF})$ deviation of ± 2 V produces a power penalty and a phase error below 1 dB and 2°, respectively. Therefore, $V_\pi(f)$ deviations may be neglected in the architecture presented in [2], but they should be considered for the architecture proposed in this letter when high-order LO harmonic are employed. Finally, it should be pointed out that the results depicted in Figure 3 correspond to a particular bias voltage value ($V_{bias1} = 1.58$), which sets a specific phase shift. Selecting different bias voltages for distinct phase shift settings results in power penalties and phase errors of slightly different values, but always remaining within ± 10 dB and $\pm 20°$, respectively, for the worst analyzed case ($N = 10$).

4. CONCLUSION

In this letter, the authors have presented a novel architecture which may be easily integrated in a photonic beam-forming feeder. This architecture performs both phase shifting and harmonic up/down-conversion of an outgoing/incoming RF signal. An investigation on the main limitation of the photonic device performance has also been provided. The results show that a maximum deviation of ± 0.5 V for the $V_\pi(f_{LO})$ parameter is tolerable when employing high LO order harmonics (up to $N = 10$), resulting in a power penalty and a phase error below 1.5 dB and 3°, respectively.

ACKNOWLEDGMENT

The authors thank the Spanish Research Commission (CICYT) for funding under Project TIC96-0611.

REFERENCES

1. J.L. Corral, J. Marti, S. Regidor, J.M. Fuster, R. Lamming, and M.J. Cole, True time delay scheme for feeding optically controlled phased array antennas using chirped fiber gratings, IEEE Trans Microwave Theory Tech 45 (1997), 1531–1536.
2. J.F. Coward, T.K. Yee, C.H. Chalfant, and P.H. Chang, A photonic integrated-optic RF phase shifter for phased array antenna beam-forming applications, J Lightwave Technol 11 (1993), 2201–2205.
3. J.M. Fuster and J. Marti, Photonic RF phase shifter for harmonic downconversion in phased array antenna beam-forming applications, Electron Lett 33 (1997), 1426–1428.
4. V. Polo, J. Marti, F. Ramos, and J.M. Fuster, Millimeter-wave optical harmonic mixer employing a single Mach-Zehnder electro-optic modulator, 28th European Microwave Conf, Amsterdam, The Netherlands, 1998, paper MD-4, pp. 81–86.

CCC 0895-2477/99

HIGHER ORDER IMPEDANCE BOUNDARY CONDITIONS FOR METAL-BACKED INHOMOGENEOUS DIELECTRIC LAYERS

Vincenzo Galdi[1] and Innocenzo M. Pinto[1]
[1] Waves Group
D. I. I. I. E.
University of Salerno
I-84084 Fisicano (SA), Italy

Received 11 February 1999

ABSTRACT: *A systematic spectral-domain approach is described for obtaining higher order electromagnetic impedance boundary conditions for isotropic, longitudinally inhomogeneous, dielectric coatings on a polarization-preserving impedance plane. Representative computational examples including single- and two-layer inhomogeneous coatings are discussed to illustrate the accuracy of the proposed approach.* © 1999 John Wiley & Sons, Inc. Microwave Opt Technol Lett 22: 249–254, 1999.

Key words: *impedance boundary conditions; electromagnetic scattering; dielectric coatings*

I. INTRODUCTION

The frequent use of nonmetallic materials and composites, often in the form of thin layered coatings laid on conducting bodies, in many microwave devices and antennas, as well as modern aircraft, demands more effective models for computing the electromagnetic field scattered by those objects.

Available numerical techniques for tackling this problem fall conceptually into two categories. Whenever the coating is (piecewise) homogeneous, one can use a combined field integral equation approach [1], leading, e.g., through the method of moments [2] to the solution of a linear matrix problem. This requires knowledge of the Green's function of the coating material, whose computation might become quite cumbersome or even impossible for complex coating materials.

In the presence of inhomogeneous dielectrics, one has to compute the fields at every point inside the coating, using, e.g., finite-element and related methods [3], featuring a considerable number of unknowns. These methods can be plagued by numerical instabilities whenever the thickness of the layer becomes very small as compared to the wavelength.

A possible approach for improving the efficiency of numerical methods for this kind of scattering problem is to use approximate impedance boundary conditions (henceforth IBCs) [4], which relate the tangential (or normal) components of the electric and magnetic fields at the interface between the coated body and free space through differential equations, and whose coefficients depend on the *local* material

and geometrical properties of the coating. The simplest and most popular version, usually known as Leontovich or standard IBC (henceforth SIBC) [5], relates the tangential electric and magnetic fields through a simple (complex) constant, and has long since been used. As is well known, SIBC is quite accurate whenever the reflection properties of the layer are *weakly* dependent on the angle of incidence, i.e., for electrically *thin* and/or significantly *lossy* layers. In order to simulate more general coatings, one has to introduce derivatives of the field components into the approximate IBCs, yielding the generalized IBCs (henceforth GIBCs) or higher order IBCs (henceforth HOIBCs) [6–8], which have been applied to a variety of scattering problems involving homogeneous [9, 10] and inhomogeneous [11, 12] dielectric layers, dielectric-filled grooves [13], and multilayer coatings [14–16].

Recently, a spectral-domain framework has been introduced by Hoppe and Rahmat-Samii [17] for systematically deriving HOIBCs for metal-backed, piecewise homogeneous coatings with arbitrary constitutive relations laid on planar as well as curved boundaries. Technically, it is based upon suitable rational approximations (in the spectral variables) of the exact spectral-domain IBCs (which always can be computed analytically), which are Fourier transformed to obtain the sought spatial-domain HOIBCs. This approach is quite general, systematic, and accurate. Therefore, it appears very well suited to be implemented in numerical codes, and has been used successfully in a number of two-dimensional [18] and three-dimensional [19] scattering problems.

In this paper, we propose a simple and effective strategy to remove one of the main restrictions of the aforementioned approach, namely, the impossibility of handling inhomogeneous coatings. To this end, we solve the canonical problem of electromagnetic scattering by an infinite polarization-preserving impedance plane coating by an isotropic, inhomogeneous (possibly lossy) dielectric layer with arbitrary permittivity profile.

We use a power-series expansion technique to solve the resulting (uncoupled) Sturm–Liouville problems, which rule the propagation inside the dielectric layer for the two possible polarizations, and derive the *exact* spectral-domain IBCs. Then, following Hoppe and Rahmat-Samii [17], we work out the sought HOIBCs by using suitable rational approximations and Fourier transformation. Generalization to multilayer coatings is straightforward.

The remainder of the paper is organized as follows. In Section II, the derivation of HOIBCs for an arbitrary isotropic, inhomogeneous dielectric coating on a polarization-preserving impedance plane is outlined. In Section III, some numerical examples involving single as well as multilayer coatings are worked out to illustrate the better accuracy of the proposed HOIBCs as compared to SIBC. Conclusions follow under Section IV. An implicit time-harmonic dependence $\exp(i\omega t)$ is assumed and suppressed throughout the paper.

II. DERIVATION OF HOIBCs

Let us consider the canonical problem of electromagnetic scattering by an infinite polarization-preserving impedance plane coated by an arbitrary isotropic, longitudinally[1] inhomogeneous (possibly lossy) dielectric layer, as depicted in Figure 1. The relative permittivity profile can be written as

[1]Here and henceforth, *longitudinal* means normal to the layer.

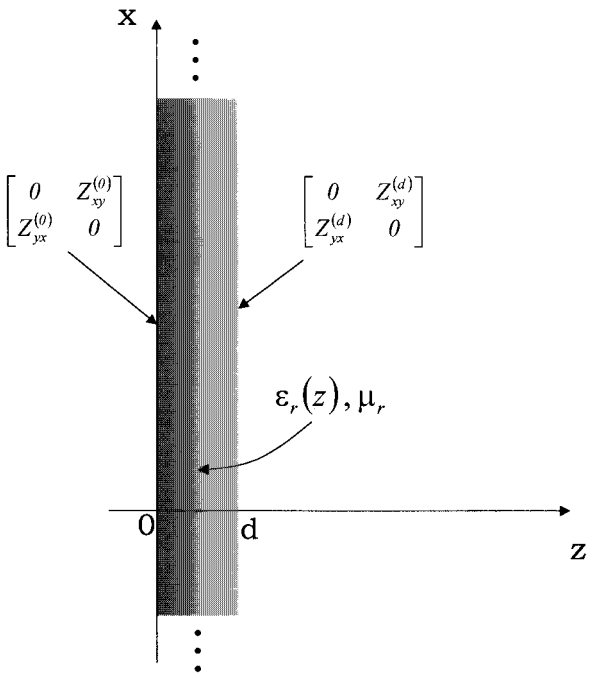

Figure 1 Impedance-plane backed inhomogeneous dielectric layer

follows:

$$\varepsilon_r(z) = \varepsilon_r^{(0)}[1 - 2\Delta f(z)] \tag{1}$$

where

$$\Delta = \frac{\varepsilon_r^{(0)} - \varepsilon_r^{(d)}}{2\varepsilon^{(0)}} \tag{2}$$

is the so-called *profile height parameter*, the function $f(z)$ is assumed to be analytic within the interval $0 \le z \le d$, and $f(0) = 0$, $f(d) = 1$, d being the layer thickness. In the following, without loss of generality, we will assume $f(z)$ monotonic and $\varepsilon_r^{(0)} > \varepsilon_r^{(d)}$.

Since the dielectric layer is uniform and infinite along the x, y directions, the x, y dependence may be written as $\exp[-i(k_x x + k_y y)]$, k_x, k_y being the transverse wavenumbers (spectral variables). This dependence henceforth will be suppressed for notational simplicity. Note that, due to the rotational invariance of the geometry under analysis, we let $k_y = 0$ to obtain the sought HOIBCs [17].

Let the impedance plane ($z = 0$) be described by polarization-preserving IBCs.

$$\begin{bmatrix} E_x(k_x, 0) \\ E_y(k_x, 0) \end{bmatrix} = \begin{bmatrix} 0 & Z_{xy}^{(0)} \\ Z_{yx}^{(0)} & 0 \end{bmatrix} \begin{bmatrix} H_x(k_x, 0) \\ H_y(k_x, 0) \end{bmatrix} \tag{3}$$

which account for the presence of a (possibly lossy) conducting surface, or represent the effect of further isotropic dielectric layers.

As already stated, our very first task consists of working out the *exact* spectral-domain IBCs at the interface $z = d$,

namely,

$$\begin{bmatrix} E_x(k_x,d) \\ E_y(k_x,d) \end{bmatrix} = \begin{bmatrix} 0 & Z_{xy}^{(d)}(k_x) \\ Z_{yx}^{(d)}(k_x) & 0 \end{bmatrix} \begin{bmatrix} H_x(k_x,d) \\ H_y(k_x,d) \end{bmatrix}. \quad (4)$$

We recall that $Z_{xy}^{(d)}(0) = -Z_{yx}^{(d)}(0)$, and that, for lossless materials, $\mathrm{Re}[Z_{xy}^{(d)}(k_x)] = \mathrm{Re}[Z_{yx}^{(d)}(k_x)] = 0$ [17]. We observe that, due to isotropy of the coating and polarization-preserving features of the impedance plane, the transverse electric (henceforth TE) and transverse magnetic (henceforth TM) components of the fields inside the coating are uncoupled. Therefore, for computing $Z_{yx}^{(d)}$, one has to consider a TE polarization (E_y, H_x, H_z), whereas a TM polarization (E_x, E_z, H_y) should be considered for computing $Z_{xy}^{(d)}$. The z-dependence of the transverse fields inside the coating is ruled by the well-known Sturm–Liouville problems [20]:

$$\left\{ \frac{\partial^2}{\partial z^2} + k_z^2 - [\varepsilon_r^{(0)} - \varepsilon_r^{(d)}]\,\mu_r k_0^2 f(z) \right\} E_y(k_x,z) = 0 \quad (5)$$

$$\left\{ \frac{\partial^2}{\partial z^2} - \frac{1}{\varepsilon_r(z)} \frac{d\varepsilon_r(z)}{dz} \frac{\partial}{\partial z} + k_z^2 - [\varepsilon_r^{(0)} - \varepsilon_r^{(d)}]\,\mu_r k_0^2 f(z) \right\} H_y(k_x,z) = 0 \quad (6)$$

under the boundary conditions (3), and

$$H_x(k_x,z) = -\frac{i}{k_0 \eta_0 \mu_r} \frac{\partial E_y(k_x,z)}{\partial z} \quad (7)$$

$$E_x(k_x,z) = \frac{i\eta_0}{k_0 \varepsilon_r(z)} \frac{\partial H_y(k_x,z)}{\partial z}. \quad (8)$$

In Eqs. (5)–(8), $k_0 = 2\pi/\lambda_0$ and η_0 denote, respectively, the free-space wavenumber and characteristic impedance, μ_r is the (constant) relative permeability, and $k_z^2 = (\varepsilon_r^{(0)}\mu_r k_0^2 - k_x^2)$.

Since, by assumption, $f(z)$ is analytic and $\varepsilon_r(z)$ does not vanish in $[0,d]$, (5) and (6) admit a convergent Taylor series solution in $0 \le z \le d$ [21].

We start with the TE case, and let

$$f(z) = \sum_{n=1}^{\infty} f_n (k_0 z)^n, \qquad E_y(k_x,z) = \sum_{n=0}^{\infty} a_n (k_0 z)^n \quad (9)$$

in the Sturm–Liouville problem (5). Differentiating repeatedly the resulting identity and setting $z = 0$, so as to equate to zero all coefficients of the resulting power series in $k_0 z$, a recursion relation for the unknown coefficients a_n is readily found [21]:

$$a_n = \frac{[\varepsilon_r^{(0)} - \varepsilon_r^{(d)}]\,\mu_r \sum_{j=1}^{n-2} f_j a_{n-j-2} - \left[\varepsilon_r^{(0)}\mu_r - \frac{k_x^2}{k_0^2} \right] a_{n-2}}{n(n-1)}, \quad n \ge 2. \quad (10)$$

The first two coefficients a_0, a_1 can be obtained as follows. Since we are interested in computing the ratio between E_y and

$$H_x(k_x,z) = -\frac{i}{k_0 \eta_0 \mu_r} \frac{\partial E_y(k_x,z)}{\partial z} = -\frac{i}{\eta_0 \mu_r} \sum_{n=1}^{\infty} n a_n (k_0 z)^{n-1}, \quad (11)$$

it follows that a_1 can be chosen arbitrarily. The remaining coefficient is determined by the boundary condition (3), viz

$$a_0 = -i \frac{Z_{yx}^{(0)} a_1}{\eta_0 \mu_r}. \quad (12)$$

For the TM case, we let

$$\frac{1}{\varepsilon_r(z)} \frac{d\varepsilon_r(z)}{dz} = k_0 \sum_{n=0}^{\infty} g_n (k_0 z)^n, \qquad H_y(k_x,z) = \sum_{n=0}^{\infty} b_n (k_0 z)^n, \quad (13)$$

from which, proceeding as for the TE case,

$$b_n = \frac{[\varepsilon_r^{(0)} - \varepsilon_r^{(d)}]\,\mu_r \sum_{j=1}^{n-2} f_j b_{n-j-2} + \sum_{j=0}^{n-1} (n-j-1) g_j b_{n-j-1} - \left[\varepsilon_r^{(0)}\mu_r - \frac{k_x^2}{k_0^2} \right] b_{n-2}}{n(n-1)}, \quad n \ge 2 \quad (14)$$

$$b_1 = -i \frac{Z_{xy}^{(0)} \varepsilon_r^{(0)} b_0}{\eta_0} \quad (15)$$

and b_0 is chosen arbitrarily.

The (insofar) exact impedance boundary conditions can be accordingly written as

$$Z_{xy}^{(d)}(k_x) = \frac{E_x(k_x,d)}{H_y(k_x,d)} = i \frac{\eta_0}{\varepsilon_r^{(d)}} \frac{\sum_{n=1}^{\infty} n b_n (k_0 d)^{n-1}}{\sum_{n=0}^{\infty} b_n (k_0 d)^n} \quad (16)$$

$$Z_{yx}^{(d)}(k_x) = \frac{E_y(k_x,d)}{H_x(k_x,d)} = -i\eta_0 \mu_r \frac{\sum_{n=0}^{\infty} a_n (k_0 d)^n}{\sum_{n=1}^{\infty} n a_n (k_0 d)^{n-1}}. \quad (17)$$

The convergence features of the *truncated* versions of (16)–(17), needed for practical evaluation, will be discussed in the following section.

Taking into account Eqs. (10) and (14), it is readily recognized that the above impedances are meromorphic functions of k_x^2. For computational purposes, as suggested in [17], they can be approximated by suitable rational functions (in k_x^2), which can be readily Fourier transformed into differential

equations in the spatial domain via $k_x \to id/dx$. In the following, we will focus our attention on second-order rational approximants, i.e.,

$$\tilde{Z}_{xy}^{(d)} = \frac{c_0 + c_1 k_x^2}{1 + c_2 k_x^2} \tag{18}$$

$$\tilde{Z}_{yx}^{(d)} = -\frac{c_0 + c_3 k_x^2}{1 + c_4 k_x^2} \tag{19}$$

where

$$c_0 = Z_{xy}^{(d)}(0) = -Z_{yx}^{(d)}(0) \tag{20}$$

and the remaining four unknown coefficients can be computed by matching the exact impedances (16)–(17) and their rational approximations (18)–(19) at two suitable different values of k_x (e.g., $k_x = 0.5\sqrt{\varepsilon_r^{(0)}}k_0, \sqrt{\varepsilon_r^{(0)}}k_0$, so as to span both the visible and the surface-wave range [17]).

Once the coefficients are computed, the spatial-domain second-order IBCs can be written as

$$\left(1 - c_2\frac{d^2}{dx^2}\right)E_x(x) = \left(c_0 - c_1\frac{d^2}{dx^2}\right)H_y(x) \tag{21}$$

$$\left(1 - c_4\frac{d^2}{dx^2}\right)E_y(x) = \left(-c_0 + c_3\frac{d^2}{dx^2}\right)H_x(x). \tag{22}$$

As remarked in [17], the above IBCs have exactly the same form as the third-order GIBCs derived in [8]. Furthermore, for rotationally invariant dielectric coatings, the general form of the second-order IBCs (i.e., $k_y \neq 0$) can be readily obtained in terms of c_k, $k = 0, \ldots, 4$, viz. [17]

$$\left(1 - c_2\frac{\partial^2}{\partial x^2} - c_4\frac{\partial^2}{\partial y^2}\right)E_x(x,y) = \left(c_0 - c_1\frac{\partial^2}{\partial x^2} - c_3\frac{\partial^2}{\partial y^2}\right)H_y(x,y) \tag{23}$$

$$\left(1 - c_4\frac{\partial^2}{\partial x^2} - c_2\frac{\partial^2}{\partial y^2}\right)E_y(x,y) = \left(-c_0 + c_3\frac{\partial^2}{\partial x^2} + c_1\frac{\partial^2}{\partial y^2}\right)H_x(x,y). \tag{24}$$

We remark that the above procedure is immediately extended to multilayer coatings, the starting ($z = 0$) impedance plane itself representing the effect of all further layers. Obviously, standard transmission-line impedance transport formulas [22] can be used in the presence of uniform layers. Extension to curved coatings (via a *locally planar* approximation) and (smooth) transverse inhomogeneities (using position-dependent coefficients) is also straightforward, as described in [17].

III. NUMERICAL RESULTS

As a first issue, we consider the truncation (in n) of the exact impedances (16)–(17). This is needed both for computing the rational-approximant coefficients (via point matching) and to construct a benchmark for checking the accuracy of the obtained HOIBCs. For our numerical simulations, we found that using $N = 100$ terms in (16)–(17) guaranteed a five-digit accuracy over a reasonably wide range of parameters for all profiles tested.

As a first example, we consider a lossless *linear* profile (i.e., $f(z) = z/d$) coating laid on a perfectly conducting plane. In Figure 2 are reported the (purely imaginary) *exact* impedances (16)–(17) and their second-order rational approximations (18)–(19) as functions of the scaled spectral variable. For this example, the matching points have been chosen to span both the visible and the surface-wave range ($k_x = 0, 0.5\sqrt{\varepsilon_r^{(0)}}k_0, \sqrt{\varepsilon_r^{(0)}}k_0$), and one obtains a uniformly high accuracy.

As a further check, we consider the scattering of a plane wave ($k_y = 0$) impinging from free space on the coated plane under analysis, as suggested in [8, 17]. The reflection coefficients can be written as (see, e.g., [17])

$$\begin{bmatrix} R_{\mathrm{TETE}} & 0 \\ 0 & R_{\mathrm{TMTM}} \end{bmatrix} = -\left([M_E] + \begin{bmatrix} 0 & Z_{xy}^{(d)} \\ Z_{yx}^{(d)} & 0 \end{bmatrix} \times [M_H]\right)^{-1} \left([M_E] - \begin{bmatrix} 0 & Z_{xy}^{(d)} \\ Z_{yx}^{(d)} & 0 \end{bmatrix}[M_H]\right) \tag{25}$$

where

$$[M_E] = \begin{bmatrix} 0 & k_{z0}/k_0 \\ 1 & 0 \end{bmatrix}, \quad [M_H] = \frac{1}{\eta_0}\begin{bmatrix} k_{z0}/k_0 & 0 \\ 0 & -1 \end{bmatrix}, \quad k_{z0} = (k_0^2 - k_x^2)^{1/2}. \tag{26}$$

Figure 3 shows the behaviors of the phase of the reflection coefficients (the magnitude being unitary for lossless coatings) as a function of the incidence angle ($\theta_i = \sin^{-1}(k_x/k_0)$) for a fixed (average) electrical length, using the exact IBCs (16)–(17), the second-order IBCs (18)–(19), and the SIBC (Eqs. (16)–(17) with $k_x = 0$). As one can see, the agreement between the results obtained using exact and second-order IBCs is excellent, whereas, as already noted in [17] for the special case of uniform coatings, SIBC gives inaccurate results.

Obviously, the accuracy provided by approximate IBCs depends on the coating parameters. In particular, as the (average) electrical length of the coating increases, the first pole in k_x-space is crossed (roughly for $\varepsilon_r^{(0)}d > 0.44\lambda_0$), and the accuracy gets substantially worse. Nevertheless, even in this case, the errors can be tolerable, due to the rational

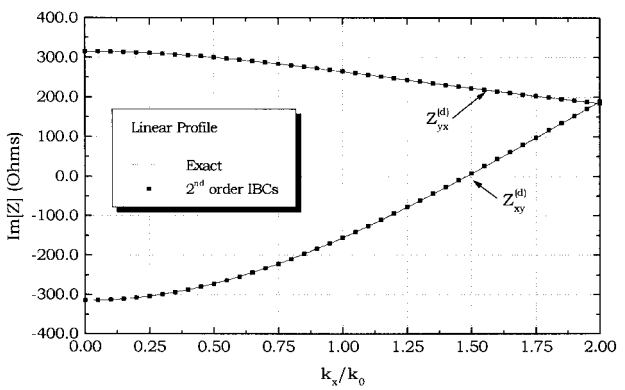

Figure 2 IBCs for a linear-profile coating with $\varepsilon_r^{(0)} = 4$, $\varepsilon_r^{(d)} = 1$, $\mu_r = 1$, $d = 0.1\lambda_0$

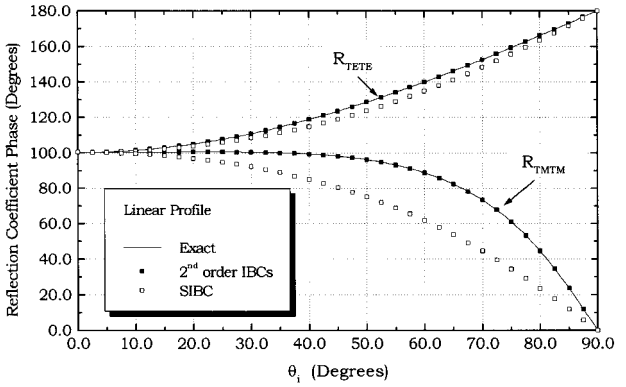

Figure 3 Phase of plane-wave reflection coefficients for a linear-profile coating with $\varepsilon_r^{(0)} = 4$, $\varepsilon_r^{(d)} = 1$, $\mu_r = 1$, $d = 0.1\lambda_0$

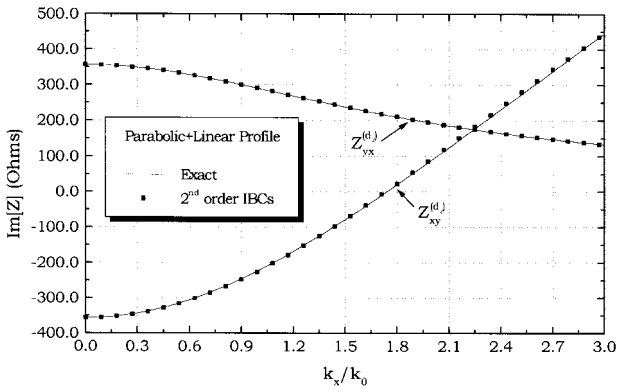

Figure 5 IBCs for a two-layer (parabolic + linear) coating with $\varepsilon_r^{(0)} = 9$, $\varepsilon_r^{(d_1)} = 3$, $\varepsilon_r^{(d_2)} = 1$, $d_1 = 0.05\lambda_0$, $d_2 = 0.1\lambda_0$

structure of the approximate IBCs, which *mimics* the pole singularity. Electrically thicker coatings would thus require IBCs of higher order.

Finally, we consider a two-layer (parabolic + linear) coating, as depicted in Figure 4. Again, in order to get a more severe test, the whole structure is assumed lossless. HOIBCs for the above coating are obtained by simply iterating the procedure illustrated in Section II. Also, in this case $k_x = 0, 0.5\sqrt{\varepsilon_r^{(0)}}\,k_0, \sqrt{\varepsilon_r^{(0)}}\,k_0$ have been chosen as matching points for computing the second-order rational approximants of the overall ($z = d_2$) IBCs. As shown in Figure 5, the exact and second-order IBCs are in excellent agreement. Therefore, second-order IBCs are adequate to simulate even the properties of this relatively complex coating. The same conclusion is drawn from the reflection coefficient phase behavior reported in Figure 6, where, again, SIBC yields quite inaccurate results.

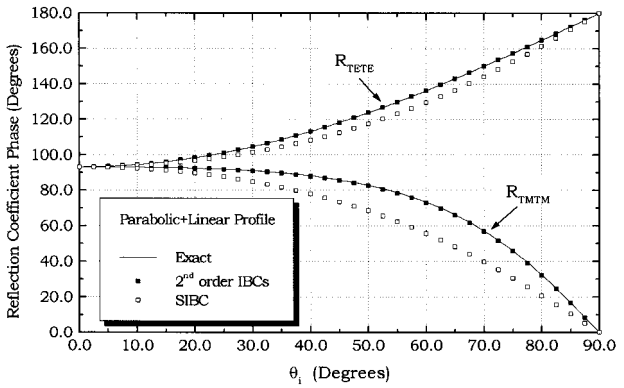

Figure 6 Phase of plane-wave reflection coefficients for a two-layer (parabolic + linear) coating with $\varepsilon_r^{(0)} = 9$, $\varepsilon_r^{(d_1)} = 3$, $\varepsilon_r^{(d_2)} = 1$, $d_1 = 0.05\lambda_0$, $d_2 = 0.1\lambda_0$

IV. CONCLUSIONS

A general spectral-domain framework for developing HOIBCs for isotropic, multilayer, inhomogeneous dielectric coatings laid on polarization-preserving impedance planes has been presented. The proposed method extends the approach recently introduced by Hoppe and Rahmat-Samii for homogeneous coatings [17]. Numerical examples show that very accurate results can be obtained by using second-order IBCs, and confirm that the method is easy and versatile, and thus very well suited for numerical implementation.

Possible extensions, presently under investigation, include (bi)anisotropic layers and curved boundaries.

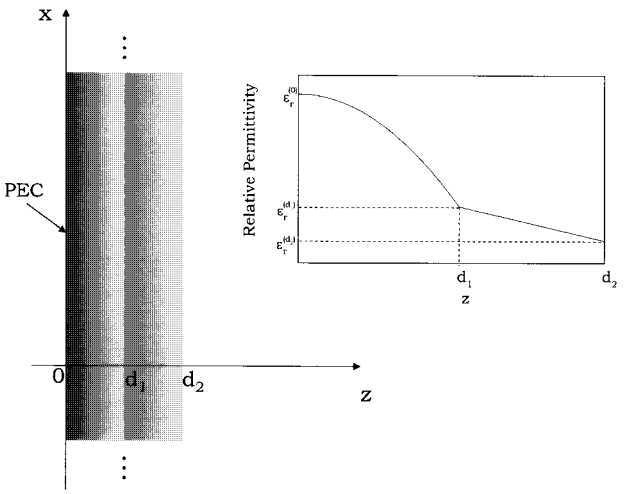

Figure 4 Two-layer (parabolic + linear) dielectric coating profile

REFERENCES

1. P.L. Huddleston, L.N. Medgyesi-Mitschang, and J.M. Putnam, Combined field integral equation formulation for scattering by dielectrically coated conducting bodies, IEEE Trans Antennas Propagat AP-34 (1986), 510–520.
2. R.F. Harrington, Field computation by moment methods, Macmillan, New York, 1960.
3. J.M. Jin and V. Liepa, Application of hybrid finite element to electromagnetic scattering from coated cylinders, IEEE Trans Antennas Propagat 36 (1988), 50–54.
4. T.B.A. Senior, Approximate boundary conditions, IEEE Trans Antennas Propagat AP-29 (1981), 826–829.
5. M.A. Leontovich, Investigations on radiowave propagation, Part II, Academy of Sciences, Moscow, Russia, 1948.
6. S.N. Karp and F.C. Karal, Jr., "Generalized impedance boundary conditions with application to surface wave structures," Electromagnetic theory, Part 1, Pergamon, New York, 1965, pp. 479–483.
7. A.L. Weinstein, The theory of diffraction and the factorization method, Golem, Boulder, CO, 1969.
8. T.B.A. Senior and J.L. Volakis, Derivation and application of a class of generalized impedance boundary conditions, IEEE Trans Antennas Propagat 37 (1989), 1566–1572.
9. J.L. Volakis and T.B.A. Senior, Sheet simulation of a thin dielectric layer, Radio Sci 22 (1987), 1261–1272.

10. J.L. Volakis and T.B.A. Senior, Application of a class of generalized boundary conditions to scattering by a metal-backed dielectric half-plane, Proc IEEE 77 (1989), 796–805.
11. H. Hammari and S. He, Generalized effective impedance boundary conditions for an inhomogeneous thin layer in electromagnetic scattering, J Electromag Waves Appl 11 (1997), 1197–1211.
12. H. Hammari and S. He, Effective impedance boundary conditions for an inhomogeneous thin layer on a curved metallic surface, IEEE Trans Antennas Propagat 46 (1998), 710–715.
13. K. Barkeshli and J.L. Volakis, TE scattering by a one-dimensional groove in a ground-plane using higher-order impedance boundary conditions, IEEE Trans Antennas Propagat 38 (1990), 1421–1428.
14. J.L. Volakis and H.H. Syed, Application of higher order boundary conditions to scattering by multilayer coated cylinders, J Electromag Waves Appl 4 (1990), 1157–1180.
15. M.A. Ricoy and J.L. Volakis, Derivation of generalized transition/boundary conditions for planar multiple-layer structures, Radio Sci 25 (1990), 391–405.
16. S.A. Tretyakov, Generalized impedance boundary conditions for isotropic multilayers, Microwave Opt Technol Lett 17 (1998), 262–265.
17. D.J. Hoppe and Y. Rahmat-Samii, Impedance boundary conditions in electromagnetics, Taylor & Francis, Washington, DC, 1995.
18. D.J. Hoppe and Y. Rahmat-Samii, Scattering by superquadric dielectric-coated cylinders using higher-order impedance boundary conditions, IEEE Trans Antennas Propagat 40 (1992), 1513–1523.
19. D.J. Hoppe and Y. Rahmat-Samii, Scattering by coated bodies of revolution using higher-order impedance boundary conditions, Proc IEEE AP-S Symp, Ann Arbor, MI, June 1993, pp. 1764–1767.
20. A.W. Snyder and J.D. Love, Optical waveguide theory, Chapman & Hall, London, England, 1983.
21. C.M. Bender and S.A. Orzag, Advanced mathematical methods for scientists and engineers, McGraw-Hill, New York, 1978.
22. R.F. Harrington, Time-harmonic electromagnetic fields, McGraw-Hill, New York, 1960.

CCC 0895-2477/99

COMPACT DUAL-FREQUENCY CIRCULAR MICROSTRIP ANTENNA WITH AN OFFSET CIRCULAR SLOT

Jui-Han Lu[1] and Kin-Lu Wong[2]
[1] Department of Electronic Communication Engineering
National Kaohsiung Institute of Marine Technology
Kaohsiung, Taiwan 811, R.O.C.
[2] Department of Electrical Engineering
National Sun Yat-Sen University
Kaohsiung, Taiwan 804, R.O.C.

Received 12 January 1999

ABSTRACT: *This paper presents a new, compact, dual-frequency design of single-feed circular microstrip antennas with an offset circular slot placed close to the patch boundary. It is found that, when the radius of the offset slot is about 0.38–0.62 times the radius of the circular patch, dual-frequency operation can be achieved using a single probe feed. The two operating frequencies have orthogonal polarization planes, and have a low frequency ratio of about 1.15–1.18. The two frequencies can also be much lower than the fundamental resonant frequency of a corresponding simple circular patch antenna without the offset slot. This behavior makes the proposed antenna have a reduced antenna size as compared to a simple circular patch antenna operated at either one of the two frequencies. Details of the antenna design and experimental results are presented.* © 1999 John Wiley & Sons, Inc. Microwave Opt Technol Lett 22: 254–256, 1999.

Key words: *microstrip antenna; dual-frequency operation*

1. INTRODUCTION

Dual-frequency operation is an important subject in microstrip antenna designs [1], and dual-frequency microstrip antennas are also attractive in mobile communications applications. Some related single-fed dual-frequency microstrip antennas with orthogonal polarization planes have also been reported [1–6]. Among these designs, the cases of using slotted rectangular microstrip antennas [4, 5] or circular microstrip antennas with a pair of inserted slits of unequal lengths [6] can also achieve compact dual-frequency operations; that is, in addition to the dual-frequency radiation, these designs have a reduced antenna size as compared to a simple rectangular or circular microstrip antenna operated at either one of the two operating frequencies. In this paper, another promising compact dual-frequency design of a circular microstrip antenna with an offset circular slot (see Fig. 1) is proposed and experimentally studied. By selecting various sizes of the circular slot, the fundamental resonant mode of TM_{11} for an unslotted circular microstrip antenna can be split into two separate resonant modes with orthogonal polarization planes. Good impedance matching of the two resonant modes can also be achieved using a single probe feed. Also, due to the circular slot embedded inside the patch, the resonant lengths of the two resonant modes are greatly increased; that is, the resonant frequencies are much lower as compared to the fundamental resonant frequency f_{11} of the unslotted circular patch antenna. A compact dual-frequency

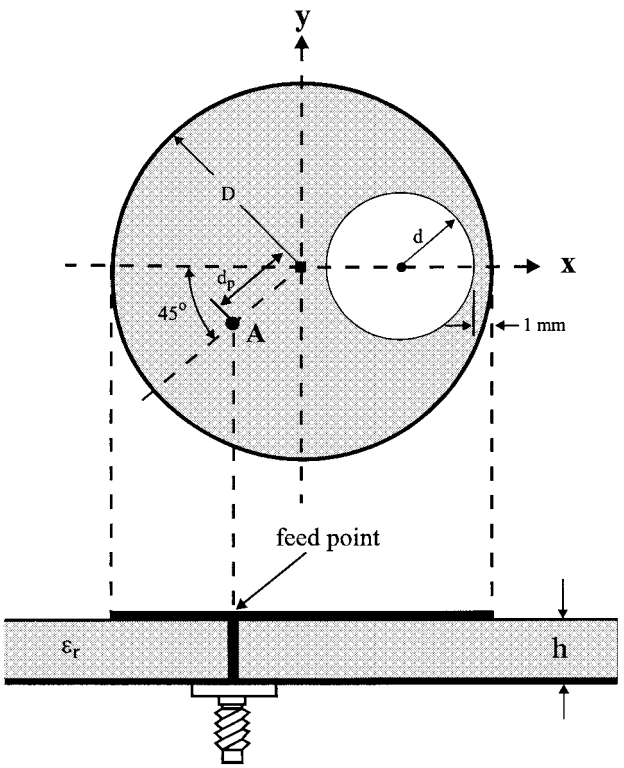

Figure 1 Geometry of a single-feed compact dual-frequency circular microstrip antenna with an offset circular slot